Clinical Neurology and Neurosurgery 115 (2013) 1317–1321

Clinical Neurology and Neurosurgery

journal homepage: www.elsevier.com/locate/clineuro

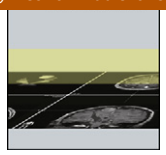

Microstructural tissue damage in normal appearing brain tissue accumulates with Framingham Stroke Risk Profile Score: Magnetization transfer imaging results of the Austrian Stroke Prevention Study

Nina Homayoon[a], Stefan Ropele[b], Edith Hofer[a,c], Petra Schwingenschuh[a], Stephan Seiler[a], Reinhold Schmidt[a,*]

[a] Department of Neurology, Division of Special Neurology, Medical University of Graz, Graz, Austria
[b] Department of Neurology, Division of General Neurology, Medical University of Graz, Graz, Austria
[c] Institute for Medical Informatics, Statistics and Documentation, Medical University of Graz, Graz, Austria

ARTICLE INFO

Article history:
Received 14 March 2012
Received in revised form
19 November 2012
Accepted 13 December 2012
Available online 6 January 2013

Keywords:
Magnetic resonance imaging
Magnetization transfer imaging
Cerebrovascular risk factors
Stroke

ABSTRACT

Background and purpose: Magnetization transfer imaging detects cerebral microstructural tissue alterations. We examined the association between the Framingham Stroke Risk Profile (FSRP) score and magnetization transfer imaging (MTI) measures in pathological and normal appearing brain tissue in clinically normal elderly subjects to determine if stroke risk leads to brain tissue destruction beyond what is visible in conventional MRI scans.
Methods: The study cohort is from the Austrian Stroke Prevention Study (ASPS). A total of 316 subjects underwent MTI and had a complete risk factor assessment sufficient to calculate the FSRP score. There were 205 women and 111 men with a mean age of 70.2 years ranging from 54 to 82 years. Subjects were grouped into four categories of stroke risk probability ranging from 3% to 88% for men and 1% to 84% for women.
Results: A higher FSRP score was significantly and independently associated with a MTR peak position shift indicating global microstructural alterations in brain tissue (BT) and in normal appearing brain tissue (NABT). The mean MTR in white matter hyperintensities (WMH) correlated inversely with increasing stroke risk. Age explained most of the variance in MTR peak position, all other risk factors of the FSRP score contributed significantly but explained an additional 2% of the variance of this MRI measure, only.
Conclusion: Increasing risk for stroke leads to microstructural brain changes invisible by standard MRI. The validity, the underlying pathogenic mechanisms and the clinical importance of these abnormalities needs to be further determined.

1. Introduction

Conventional MRI detects accumulation of brain tissue destruction with advancing age and increased stroke risk [1]. "Silent" lesions include white matter abnormalities, lacunes and less commonly thromboembolic infarcts [2,3]. Recent diffusion tensor imaging (DTI) studies reported increased stroke risk to result in microstructural cerebral damage invisible on standard MR scans. The data show an association between blood pressure and white matter microstructure integrity in several regions of the brain in healthy adults [4]. Accordingly, Kennedy and Raz [5] reported that increasing pulse pressure leads to loss of anterior white matter integrity and another investigation by Gons et al. [6] revealed that hypertension-related DTI changes in normal appearing white matter preceeded morphological lesion. Microstructural tissue alterations are not only detectable by DTI but also by magnetization transfer imaging (MTI). MTI is based on the exchange of magnetization between tissue water and protons that are bound to macromolecules such as myelin lipids and proteins. The rate of exchange gives an estimate of the magnitude of these compartments, such as the pool of bound protons. The efficacy of magnetization transfer is usually quantified by the magnetization transfer ratio (MTR) which is considered to largely reflect the myelin content of the investigated brain regions [7]. MTR decreases with advancing age. As to whether stroke risk per se also leads to MTR-detectable microstructural brain changes is widely unknown. We hypothesized that an increased Framingham Stroke Risk Profile Score (FSRP) which estimates the 10-year probability for incident stroke in stroke-free individuals [8] relates to a decrease in MTR metrics of normal appearing brain tissue (NABT) independently of

* Corresponding author at: Department of Neurology, Medical University of Graz, Auenbruggerplatz 22, 8063 Graz, Austria. Tel.: +43 316 385 83397; fax: +43 316 385 14178.
E-mail address: reinhold.schmidt@medunigraz.at (R. Schmidt).

0303-8467
http://dx.doi.org/10.1016/j.clineuro.2012.12.016

concomitant visible tissue damage. We tested this hypothesis in a sample of 316 participants of the Austrian Stroke Prevention Study.

2. Methods

2.1. Subjects

The study cohort consists of participants of the Austrian Stroke Prevention Study (ASPS) a single-center prospective follow-up study in residents of the city of Graz, Austria. The ASPS examines the frequency of cerebrovascular risk factors and their effect on cerebral morphology and function in the normal elderly. The study design and methods have been described previously [9,10]. On the basis of a structured clinical interview and a physical and neurologic examination, participants were free of overt neurologic or psychiatric disease including previous cerebrovascular attacks and dementia. A randomly selected sub-sample of 1073 ASPS participants took part in neuroimaging studies including brain MRI. Enrollment into the MR study of ASPS was started in 1991. Between 2001 and 2005 MTI was added to the scanning protocol. During this time period a total of 372 subjects entered the study. All of them underwent MTI. For the current investigation we included those 316 subjects (205 women, 111 men; mean age 70.2 years; range 54–82 years) who underwent both MTI scanning and a complete risk factor assessment according to the FSRP. The study protocol was approved and accepted by the ethics committee of the Medical University of Graz, Austria, and informed consent was obtained from all study participants.

2.2. Vascular risk factors

Risk factors were determined based on the participants' history and findings at the examination as previously described [10]. Diabetes was considered if a subject was treated for diabetes at the time of examination or if the fasting blood glucose level was above 126 mg^{-1} dl^{-1} at the time of examination. Blood pressure was measured by a random-zero sphygmomanometer, after 5 min of rest, and at the end of the study visit. The mean of the two measurements was used. Subjects were classified as former, current smokers or non-smokers. Cardiac disease was assumed to be present if there was an evidence of cardiac abnormalities known to be a source of cerebral embolism, evidence of coronary heart disease according to the Rose questionnaire or appropriate ECG findings (Minnesota codes: III, 1–3, IV, 1–3; or V, 1–2) or if individual presented signs of left ventricular hypertrophy on echocardiography or ECG (Minnesota codes: III, 1; or IV, 1–3). Atrial fibrillation was diagnosed based on electrocardiogram findings obtained at the study visit.

2.3. Framingham Stroke Risk Profile (FSRP)

The Framingham stroke risk predicts the probability of incident strokes within 10 years in stroke-free individuals and was calculated as described [8]. Briefly, the risk factors included in the FSRP are age, systolic blood pressure, use of antihypertensive medication, diabetes, smoking status, cardiovascular disease, atrial fibrillation, and left ventricular hypertrophy. The FSRP provides specific risk estimates for men and women. The score ranges from 1 to 30 points for men and 1 to 27 points for women. The sex-specific score is then converted to 10 year probability of strokes ranging from 3% to 88% for men and 1% to 84% for women.

2.4. Conventional MRI

The MRI methodology used in the Austrian Stroke Prevention Study has been described [10,11]. MRI was performed on 1.5-T magnets (Gyroscan S 15 and ACS, Philips, Eindhoven, The Netherlands) using proton density- and T2-weighted sequences (repetition time [TR]/echo time [TE], 2000–2500 ms/30–90 ms) in the transverse orientation. T1-weighted images (TR/TE, 600/30 ms) were generated in the sagittal plane. The slice thickness was 5 mm and the image matrix was 128 × 256 pixels. The scanning plane was always determined by a sagittal and coronal pilot scan to ensure consistency in image angulation throughout the study [10]. White matter hyperintensities (WMH) were specified and graded by the Fazekas Score [12] into absent (grade 0) punctuate (grade 1), early confluent (grade 2) and confluent (grade 3) WMH, and semiautomated WMH volume measurements were done as described in previous publications [13]. Scans were also analyzed for the presence of clinically silent cortical infarcts and lacunes. Cortical infarcts were lesions that had consistent signal characteristics involving the cortex and following a typical branch pattern [14,15]. Lacunes were focal lesions isointense to CSF involving the basal ganglia, the white matter, the internal capsule, the thalamus or the brainstem ranging in maximal diameter between 3 mm and 10 mm [16].

2.5. Magnetization transfer imaging (MTI)

MTI was performed after conventional MR imaging with a spoiled 3D gradient-echo sequence (TE = 4 ms, TR = 26 ms, FA = 20°, section thickness = 3 mm, FOV = 250 mm, matrix = 256 × 256) with and without a binomial saturation pulse (90–180–90°, maximum amplitude = 21 μT) covering the whole brain. MTR maps were calculated according to the formula MTR = (Mss-Mo)/Mo, where Mss and Mo are the signal intensities obtained with and without MT saturation, respectively. Then they were registered to the FLAIR scans using an automated affine registration tool (FLIRT, FMRIB Image Analysis Group Oxford).

MTR metrics were assessed for the whole brain tissue (BT) including the cerebellum and the brain stem. They were also recorded in normal appearing brain tissue (NABT) which was all brain tissue outside WMH and lacunes as well as for WMH. The definition of NABT and assessment of WMH were based on FLAIR scans. A mean MTR was calculated for each WMH by masking the registered MTR maps with the WMH masks. To reduce partial volume effects, which might have taken place due to image registration and subsequent interpolation, we eroded all WMH masks by 1 pixel. The MTR of all WMH was averaged to obtain a mean lesional MTR for each subject. MTR data in WMH follow a Gaussian distribution. Therefore mean MTR is the appropriate measure to describe lesional MTR data. To analyze the MTR metrics of NABT and BT, MTR maps were masked out with the WMH masks after dilating them by 1 pixel and after removing nonbrain tissue with a brain extraction tool (BET as a part of FSL, http://www.Fmnb.ox.ac.uk/fsl/bet2/index.html). All remaining voxels in the MTR maps were then considered for the MTR histogram analysis. For each histogram, we calculated the peak position (i.e. the MTR value with the highest frequency) and the relative peak height (i.e. the relative voxel count at the peak position). Mean MTR in NABT is not displayed because the MTR histogram of this tissue compartment does not follow a Gaussian distribution. To correct for differences in individual brain volumes, we normalized the histograms by the total number of voxels contributing to the histogram [17,18].

2.6. Statistical analysis

Multiple linear regression analysis was used to correlate the FSRP score with MTR metrics. The analyses were adjusted for presence of lacunes, and cortical infarcts as well as for white matter hyperintensity volume. In separate analyses adjustment was also done for number of lacunes and cortical infarcts. For each regression coefficient, the 95% confidence interval and the *p*-value were

Table 1
Demographics, risk factors and MRI findings in categories of increasing Framingham Stroke Risk Profile Scores.

	Category 1	Category 2	Category 3	Category 4
10-year stroke risk probability, %	<11	11–20	21–30	>30
N	73	110	63	70
A. Risk factors				
Age, years	66.8 ± 5.8	69.8 ± 5.8	71.4 ± 5.8	73.8 ± 5.3
Sex w/m, *N* (%)	39/34 (53.4/46.6)	70/40 (63.6/36.4)	44/19 (69.8/30.2)	52/18 (74.3/25.7)
Systolic blood pressure, mm Hg	129.6 ± 27.9	145.2 ± 19.2	162.1 ± 19.3	169.8 ± 22.8
Diabetes mellitus, *N* (%)	3 (4.6)	7 (6.4)	7 (11.1)	25 (35.7)
Cigarette smoking, *N* (%)	18 (24.7)	37 (33.6)	24 (38 .1)	32 (45.7)
Cardiovascular disease, *N* (%)	4 (5.5)	26 (23.6)	26 (41.3)	51 (72.8)
Atrial fibrillation, *N* (%)	0	0	1 (1.6)	12 (17.1)
Left ventricular hypertrophy, *N* (%)	0	1 (0.9)	2 (3.4)	5 (7.6)
Antihypertensive therapy, *N* (%)	6 (8.2)	30 (27.3)	30 (47.6)	47 (67.1)
B. MRI				
WMH, cm^3, mean ± SD (range)	1.8 ± 3.5 (0–23.4)	4.8 ± 9.9 (0–78)	4.2 ± 5.3 (0–21.4)	6.5 ± 9.2 (0–52.5)
Presence of lacunes, *N* (%)	6 (9.2)	5 (4.6)	3 (4.8)	7 (10.1)
Number of lacunes, mean ± SD (range)	0.1 ± 0.3 (0–2)	0.1 ± 0.8 (0–6)	0.0 ± 0.3 (0–2)	0.2 ± 0.7 (0–5)
Presence of cortical infarcts, *N* (%)	1 (1.5)	5 (4.5)	0	4 (5.8)
Number of Cortical infarcts, mean ± SD (range)	0.0 ± 0.1 (0–1)	0.0 ± 0.3 (0–3)	0	0.0 ± 0.2 (0–1)

Data are mean ± SD, *N* (%), percentages are based on the individual categories. Risk factors defined in the text. MRI, Magnetic Resonance Imaging; WMH, White Matter Hyperintensities; SD, standard deviation.

determined. Three different models were assessed for NABT, BT, and WMH. The first model contained the 10-year probability of stroke risk as the independent variable.

For model 2, all subjects were grouped into four categories depending on their stroke risk probability, <11% (category 1), 11–20% (category 2), 21–30% (category 3) and >30% (category 4). The characteristics of participants in each category are shown in Table 1. These categories were used as explanatory variables to determine a possible dose–response relationship. The third model included each single risk factor to assess its independent contribution on MTR metrics. For significantly related risk factors the proportion of MTR variance explained by the given risk factor was determined. We also identified the proportion of variance that is explained by all the other risk factors compiled when the most significant risk factor is already in the model. Therefore, the difference between the adjusted coefficients of determination (R^2) of model 3 and a model including only the given risk factor was computed. An *F*-test was used to assess the significance of R^2 and the change in R^2. As the study is explorative, no corrections for multiple testing have been made [19]. All analyses were performed using Stata (Stata Statistical Software, release 6; StataCorp, College Station, TX). A two-sided *p*-value <0.05 was considered to be statistically significant.

3. Results

As can be seen from Table 2, the FSRP score was significantly and independently associated with MTR peak position but not with peak height in BT and in NABT. A higher FSRP score shifted the MTR peak to the left. The associations remained virtually unchanged when adjustment was made for number of cortical infarcts and number of lacunes instead of presence or absence of these lesions. A higher FSRP score was also related to decreased mean MTR in WMH. Fig. 1 demonstrates the association between categories of increasing stroke risk and MTR peak position in BT and NABT, as well as mean MTR in WMH. The figure reveals an almost linear inverse relationship between increasing risk of stroke and MTR metrics.

When considering the relationship between the single components of the FSRP and MTR peak position and we identified age as the only significant risk factor for the shift in MTR peak position in BT and NABT (data not shown). Systolic blood pressure was not related to MTR metrics when used as a continuous variable but when the quartile distribution of systolic blood pressure was used the associations with peak position in BT and NABT became significant (*p* for trend <0.014 and <0.02, respectively). An inverse relationship with MTR peak position was only seen at systolic blood pressure values ≥151 mm Hg. Age explained the majority of the total variance in MTR peak position. The contribution of the remaining FSRP risk factors was statistically significant. They explained only 2% of the variance beyond what was explained by age alone (Table 3).

Table 2
Multiple linear regression analysis[a]: FSRP and MTR metrics in different tissue segments.

	β	95% CI	*p*
MTR in BT			
Peak position	−0.022	[−0.032, −0.013]	<0.001
Peak height	−3.36e−5	[−7.4e−5, 6.5e−6]	0.1
MTR in NABT			
Peak position	−0.021	[−0.031, −0.012]	<0.001
Peak height	−3.04e−5	[−7.0e−5, 9.5e−6]	0.135
MTR of WMH			
Mean	−0.025	[−0.044, −0.006]	0.011

Small numbers are displayed in exponential format. FSRP, Framingham Stroke Risk Profile; MTR, Magnetization Transfer Ratio; BT, Brain Tissue; NABT, normal appearing brain tissue; WMH, White Matter Hyperintensities. *β*, regression coefficient; CI, confidence interval.

[a] Adjusted for presence of lacunes, cortical infarcts, white matter hyperintensities volume.

4. Discussion

Our data show that increasing stroke risk correlates with the severity of MTI-detected microstructural tissue changes in BT, NABT and WMH in middle-aged and elderly subjects without clinical signs or symptoms of neurologic disease. Higher FSRP scores shifted the MTR peak to the left without affecting peak height. The

Table 3
Proportion of total variance in peak position in BT and NABT explained by age alone and explained by all the other FSRP risk factors together (beyond the age explained variance).

	BT	NABT
Age[a]	17% (*p*-value < 0.001)	15% (*p*-value < 0.001)
FSRP risk factors except age	2% (*p*-value = 0.029)	2% (*p*-value = 0.035)

FSRP, Framingham Stroke Risk Profile; BT, Brain Tissue; NABT, normal appearing brain tissue.

[a] Adjusted for presence of lacunes, cortical infarcts, white matter hyperintensities volume. Risk factors defined in the text.

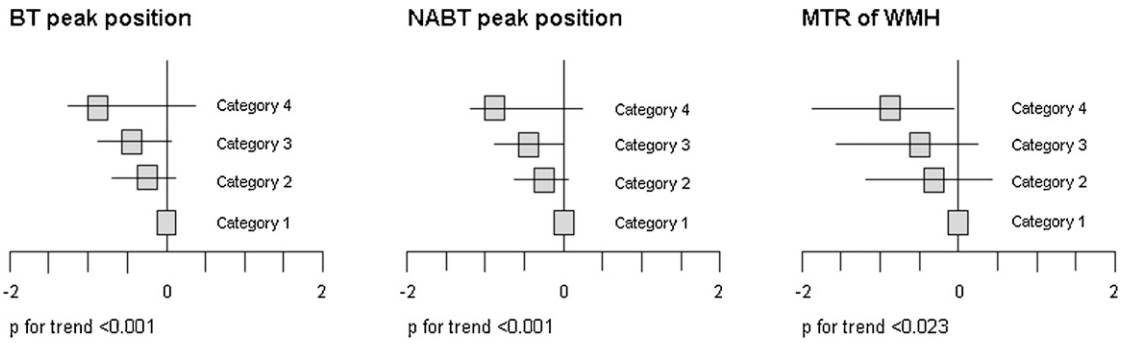

Fig. 1. Relationship between MTR peak position in BT (left panel) and NABT (middle panel) as well as MTR of WMH (right panel), and the categories of stroke risk probability (indicated on the *y*-axis). Regression analysis with the categories coded as dummy variables shows a left shift of the MTR peak in higher categories compared to category 1 in BT peak position (category 2: $\beta = -0.25$, 95% CI [−0.64 to 0.13]; category 3: $\beta = -0.39$, 95% CI [−0.83 to 0.04]; category 4: $\beta = -0.80$, 95% CI [−1.22 to −0.34]), and NABT peak position (category 2: $\beta = -0.29$, 95% CI [−0.69 to 0.09]; category 3: $\beta = -0.41$, 95% CI [−0.85 to 0.03]; category 4: $\beta = -0.81$, 95% CI [−1.25 to −0.37]) as well as a decrease in WMH MTR (category 2: $\beta = -0.36$, 95% CI [−1.18 to 0.44]; category 3: $\beta = -0.76$, 95% CI [−1.66 to 0.12]; category 4: $\beta = -0.94$, 95% CI [−1.85 to −0.04]). The squares on the *x*-axis indicate the β-coefficients and the bars indicate 95% CIs.

effect was predominantly age-related, major vascular risk factors contributed significantly but their joint effect on MTR peak position was small.

Peak height and peak position together provide complementary views on microstructural tissue changes. The peak in the histogram represents the largest tissue component, i.e. white matter. The peak height therefore reflects the relative number of voxels representing white matter [20]. Consequently, a decrease in peak height indicates focal tissue changes rather than global and diffuse alterations. By contrast, peak position is indicative of global and diffuse changes in the white matter. A shift to the left in BT and NABT as seen in our study suggests a global decrease of MTR in the white matter with demyelination being the most likely histopathological correlate [7].

Previous studies reported that the FSRP and cardiovascular risk factors were related to white matter hyperintensities volume [2] and the Framingham Offspring Study showed a positive correlation with silent cerebral infarcts [3].

Our study extents these results as we have shown that increasing stroke risk does not only lead to structural but also to microstructural tissue destruction as determined by MTI. This finding is corroborated by a previous report relating hypertension and diabetes to MTR metrics in NABT [18]. Importantly, a higher FSRP was also related to a decreased MTR in WMH indicating that the risk profile of study participants also influenced the severity of tissue destruction in ischemic lesions visible on standard MRI sequences.

Our study has several strengths. We included a large number of healthy study participants and used a MTI protocol including a 3D sequence with a high repetition rate of the MT saturation pulses. We used ultra short (1 ms) binomial MT saturation pulses and short interpulse delay, which produce a higher saturation effect. Our study design was prospective and we used a standardized protocol. Limitations of our investigation are its cross sectional design and the relative small variability of MTR metrics occurring in asymptomatic individuals. Because of the limited resolution, we refrained from segmenting the cortex as this would have otherwise introduced partial volume effects.

The validity, the underlying pathogenic mechanisms and the clinical importance of microstructural brain abnormalities in the wake of an increased stroke risk score needs to be further explored. We realize full well that the FSRP can only be considered as a surrogate of stroke risk, and a longitudinal study design would have been necessary to determine the actual risk for stroke in our study participants. A longitudinal design will also clarify the sequence of MRI findings in relation to clinical symptoms. We hypothesize that microstructural changes occur at the earliest risk stages followed by visible clinically silent brain abnormalities and ultimately clinical symptoms. Our study results that FSRP risk components were significantly related to MTR metrics but explained only 2% of their variance suggest a rather limited role of this method in the prediction of future stroke risk.

Conflict of interest

The authors declare that they have no conflict of interest.

Acknowledgement

This work was supported by the Austrian Science Fund projects (P20103 and I904).

References

[1] Schmidt R, Schmidt H, Haybaeck J, Loitfelder M, Weis S, Cavalieri M, et al. Heterogeneity in age-related white matter changes. Acta Neuropathologica 2011;122(2):171–85.
[2] Jeerakathil T, Wolf PA, Beiser A, Massaro J, Seshadri S, D'Agostino RB, et al. Stroke risk profile predicts white matter hyperintensity volume: the Framingham Study. Stroke 2004;35(8):1857–61.
[3] Das RR, Seshadri S, Beiser AS, Kelly-Hayes M, Au R, Himali JJ, et al. Prevalence and correlates of silent cerebral infarcts in the Framingham offspring study. Stroke 2008;39(11):2929–35.
[4] Salat DH, Williams VJ, Leritz EC, Schnyer DM, Rudolph JL, Lipsitz LA, et al. Inter-individual variation in blood pressure is associated with regional white matter integrity in generally healthy older adults. Neuroimage 2012;59(1):181–92.
[5] Kennedy KM, Raz N. Pattern of normal age-related regional differences in white matter microstructure is modified by vascular risk. Brain Research 2009;1297:41–56.
[6] Gons RA, de Laat KF, van Norden AG, van Oudheusden LJ, van Uden IW, Norris DG, et al. Hypertension and cerebral diffusion tensor imaging in small vessel disease. Stroke 2010;41(12):2801–6.
[7] Schmierer K, Scaravilli F, Altmann DR, Barker GJ, Miller DH. Magnetization transfer ratio and myelin in postmortem multiple sclerosis brain. Annals of Neurology 2004;56(3):407–15.
[8] D'Agostino RB, Wolf PA, Belanger AJ, Kannel WB. Stroke risk profile: adjustment for antihypertensive medication. The Framingham Study. Stroke 1994;25(1):40–3.
[9] Schmidt R, Lechner H, Fazekas F, Niederkorn K, Reinhart B, Grieshofer P, et al. Assessment of cerebrovascular risk profiles in healthy persons: definition of research goals and the Austrian Stroke Prevention Study (ASPS). Neuroepidemiology 1994;13(6):308–13.
[10] Schmidt R, Fazekas F, Kapeller P, Schmidt H, Hartung HP. MRI white matter hyperintensities: three-year follow-up of the Austrian Stroke Prevention Study. Neurology 1999;53(1):132–9.
[11] Enzinger C, Fazekas F, Matthews PM, Ropele S, Schmidt H, Smith S, et al. Risk factors for progression of brain atrophy in aging: six-year follow-up of normal subjects. Neurology 2005;64(10):1704–11.
[12] Fazekas F, Kleinert R, Offenbacher H, Schmidt R, Kleinert G, Payer F, et al. Pathologic correlates of incidental MRI white matter signal hyperintensities. Neurology 1993;43(9):1683–9.

[13] Fazekas F, Strasser-Fuchs S, Schmidt H, Enzinger C, Ropele S, Lechner A, et al. Apolipoprotein E genotype related differences in brain lesions of multiple sclerosis. Journal of Neurology, Neurosurgery and Psychiatry 2000;69(1):25–8.
[14] Schmidt R, Fazekas F, Hayn M, Schmidt H, Kapeller P, Roob G, et al. Risk factors for microangiopathy-related cerebral damage in the Austrian stroke prevention study. Journal of the Neurological Sciences 1997;152(1):15–21.
[15] Kertesz A, Black SE, Tokar G, Benke T, Carr T, Nicholson L. Periventricular and subcortical hyperintensities on magnetic resonance imaging. 'Rims, caps, and unidentified bright objects'. Archives of Neurology 1988;45(4):404–8.
[16] FISHER CM. Lacunes: small, deep cerebral infarcts. Neurology 1965;15: 774–84.
[17] Fazekas F, Ropele S, Enzinger C, Gorani F, Seewann A, Petrovic K, et al. MTI of white matter hyperintensities. Brain 2005;128(Pt 12):2926–32.
[18] Ropele S, Enzinger C, Sollinger M, Langkammer C, Wallner-Blazek M, Schmidt R, et al. The impact of sex and vascular risk factors on brain tissue changes with aging: magnetization transfer imaging results of the Austrian stroke prevention study. American Journal of Neuroradiology 2010;31(7):1297–301.
[19] Bender R, Lange S. Adjusting for multiple testing – when and how? Journal of Clinical Epidemiology 2001;54(4):343–9.
[20] Tofts P, Steens S, van Buchem M. MT: magnetization transfer. In: Paul S, Tofts, editors. Quantitative MRI of the brain. Measuring changes caused by disease. Chichester: John Wiley and Sons; 2003. p. 257–98.